

NASA Technical Memorandum 87815

Dynamic Evolution of the Source Volumes of Gradual and Impulsive Solar Flare Emissions

M. E. Bruner

*Lockheed Palo Alto Research Laboratory
Palo Alto, California*

C. J. Crannell and F. Goetz

*Goddard Space Flight Center
Greenbelt, Maryland*

A. Magun

*University of Bern
Bern, Switzerland*

D. L. McKenzie

*The Aerospace Corporation
Los Angeles, California*



National Aeronautics
and Space Administration

Scientific and Technical
Information Division

1988

PREFACE

Multiwave observations from a NASA satellite, an Air Force satellite, and two groundbased observatories are employed to investigate the dynamic source volumes of solar flares. The authors gratefully acknowledge Dr. U. Feldman and Dr. G. Doschek for providing the *P78-1* data and for discussions about the analysis of the soft X rays, Mr. K. Smith for help in the analysis of the FCS data, and Dr. R. Canfield for valuable conversations and advice for the interpretation of the results. This work was supported in part by the Lockheed Independent Research Program, contracts NAS5-24119 and NAS5-29342, NASA RTOP 188-38-01-04 and SMM Guest Investigator Project 370-04-40-02, the Aerospace Sponsored Research Program, and the Swiss National Science Foundation grant 2.241-0.86SR. During this effort, F. Goetz held a fellowship from the National Research Council of the National Academy of Sciences and fellowship number 82.375.0.86 from the Swiss National Science Foundation.

PRECEDING PAGE BLANK NOT FILMED

1 INTRODUCTION

Of the flares selected for study by the "Energetics" team of the *Solar Maximum Mission Flare Workshop* (Wu *et al.*, 1986), one event is unique in the extent of its multi-wavelength coverage and its potential for comprehensive solar-flare diagnostics. For this event on 1980 April 8, observations of the density-sensitive line complex from O VII were obtained with the SOLEX instrument on board the *P78-1* satellite; images of the O VIII, Ne IX, Mg XI, Si XIII, S XV, and Fe XXV emission sources were obtained with the Flat Crystal Spectrometer (FCS) on board the *Solar Maximum Mission* (SMM) satellite; hard X-ray images and spectra were obtained with the Hard X-ray Imaging Spectrometer (HXIS) and the Hard X-Ray Burst Spectrometer (HXRBS), respectively, also on board SMM, and microwave observations were obtained with the Toyokawa Radio Observatory. The volume of the O VII source as a function of time throughout the duration of this soft X-ray emission had been determined by Doschek *et al.* (1981) from the density and emission measure of the 2×10^6 K plasma. As part of the workshop effort, the effective source volume of the associated impulsive emissions was estimated over the same time interval from a coincident analysis of the hard X-ray and microwave observations.

The initial comparison of these source volumes, as they evolved throughout the flare, implied some intriguing relationships between the dynamics of their respective sources. Early in the flare, the impulsive source was observed to be more than 1000 times larger than the source of O VII emission. The volume of the O VII source dropped sharply just as the impulsive source volume began to increase, then gradually rose several orders of magnitude until it was comparable to the impulsive source volume. These observations are illustrated in Figure 1, taken from the SMM workshop proceedings (Wu *et al.*, 1985 p. 5-17). The dynamic evolution of the volumes calculated from the hard X-ray/microwave analysis is similar to that of the hard X-ray source areas observed with HXIS and quantitatively consistent in the context of realistic loop geometries.

The purpose of this effort is to investigate how the dynamics of the diverse flare components are related for the 1980 April 8 event from an analysis of all the observations available and then to learn if these results

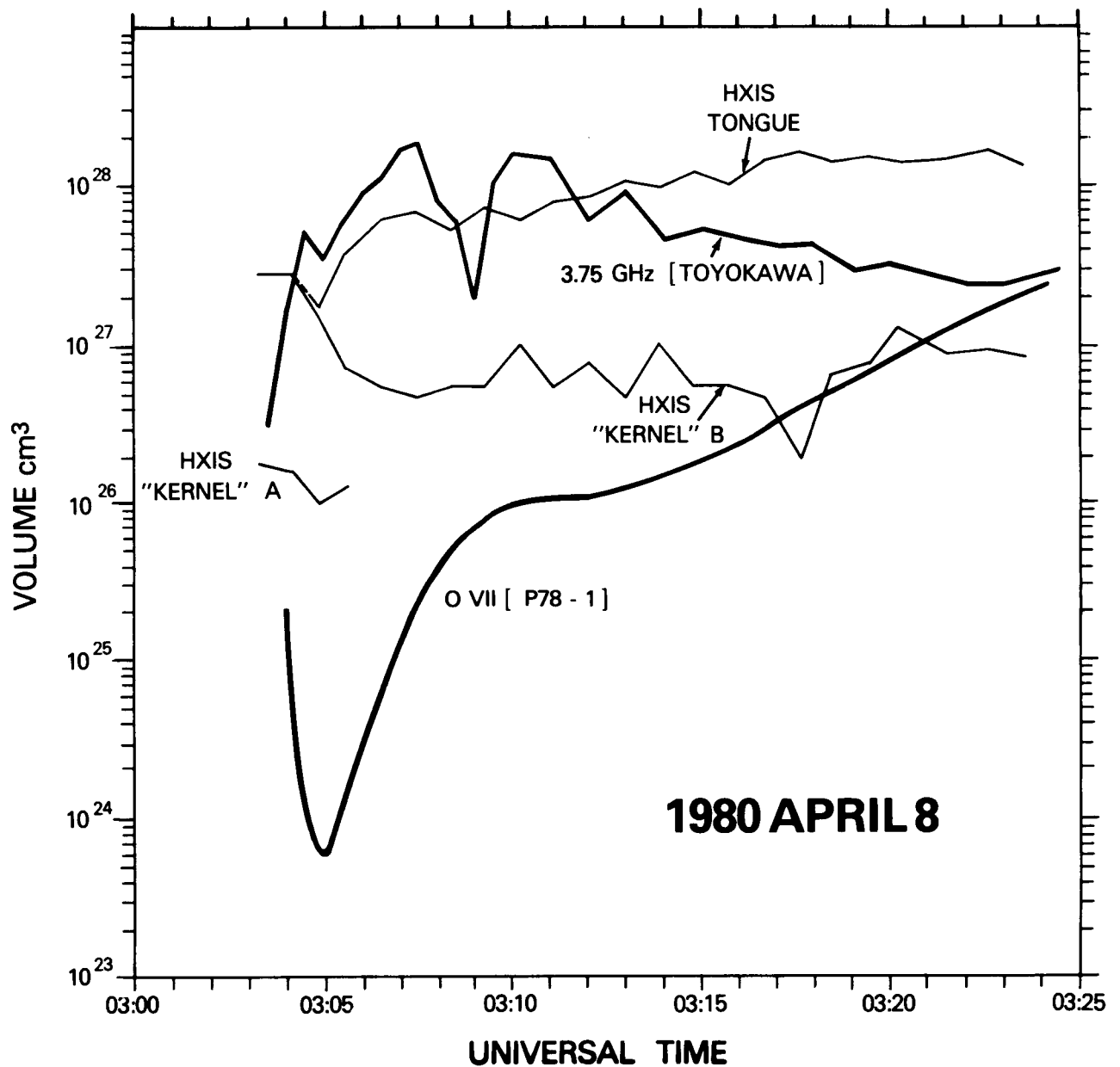


Figure 1. Source volumes for the 1980 April 8 flare determined from the HXIS soft X-ray images, the P78-1 density-sensitive line data, and the hard X-ray/microwave analysis discussed in the text. This Figure is taken from Chapter 5 (*Wu et al. 1986*) of the SMM workshop proceedings.

are typical for the analysis of such observations for other flares. *SMM* and *P78-1* data were searched for more flares with similar observational coverage. Two such flares were found: the first occurred on 1980 May 9 and the second, on 1981 February 26. The observations of these three events comprise the data for the present work.

The results from the analysis of these three events reveal striking similarities in their dynamic behavior. In each of the events the hard X-ray/microwave source volume rose in a time commensurate with the rise of the impulsive emissions but decreased on a much more gradual time scale. The apparent sharp drop in the O VII source volume observed for the April 8 event occurred in the other two events as well and in each case this volume reached a minimum at approximately the same time as the peak in the impulsive source volume. Each of the events also exhibited a rise in the O VII volume after the peak in the impulsive emissions. The volumes of the May 9 and February 26 events, however, attained plateau values that were nearly an order of magnitude smaller than the peak impulsive volume. These observations, taken together with the reports of blue shifts for each of the three events, suggest that the soft X-ray emissions are manifestations of heating by the electrons comprising the source of the hard X rays and microwaves. Thus, the results of this investigation suggest a scenario in which energetic electrons, confined in a magnetic loop, produce not only the impulsive flare emissions but also are responsible for heating the ambient material at the loop footpoints producing the gradual flare components.

Analysis of the observations and physical assumptions underlying the calculation of model-dependent parameters are described in the following section. Detailed results for the analysis of the dynamical behavior of source size and density for each of the three flares are presented in Section 3. The conclusions that can be drawn from these results are discussed and summarized in Section 4.

2 ANALYSIS

In the present work, observations of the 1980 April 8 flare were reanalyzed so that results for both thermal and nonthermal interpretations of the impulsive emissions could be compared directly. The O VII line emission for this event also was reanalyzed, making use of refinements of the SOLEX response function, and of more recent theoretical calculations that enable the determinations of temperature, density, and emission measure of the O VII source. The results from this analysis were compared to soft X-ray imaging observations obtained with the Flat Crystal Spectrometer (FCS) on board the *SMM*. These data consist of a sequence of raster images obtained throughout the event with each of the six FCS detectors. The images were deconvolved with the instrument response function, and two sources of radiation were resolved in agreement with what was expected from the analysis of the other observations. Measurements of the source areas for O VIII, Ne IX, Mg XI, and Si XIII made it also possible to estimate the area, and thickness, of the source of O VII emission.

Observations of the flares of 1980 May 9 and 1981 February 26 were obtained with the Hard X-Ray Burst Spectrometer (HXRBS) on board the *SMM*, and with the solar radio observatory in Bern, Switzerland. X rays with energies up to 200 keV were detected for the May 9 event, and up to 300 keV for the February 26 event. During both flares, microwave fluxes were measured at 5.2, 8.4, 11.8, 19.6 and 35 GHz. For these flares also, observations of the density-dependent O VII line emission were obtained with the SOLEX instrument on board *P78-1*. No soft X-ray imaging observations were available for these two events.

In the case of all three flares, a discussion of the soft X-ray emission resulting from the active-region background has led to two different estimates of the O VII source densities and volumes. The comparison between these two is important for the interpretation developed in the following sections.

2.1 The Hard X-ray/Microwave Analysis

This coincident analysis of the hard X rays and microwaves is based on the assumption that the effective temperature of the microwave source

can be approximated by the temperature determined from the spectrum of the associated hard X-ray emission. This is suggested by the similarity, often observed during flares, between the time-intensity profiles of hard X rays and microwaves, especially in the optically thin part of the spectrum. In Figures 2 and 3, the time histories of hard X rays and of microwaves at 8.4 GHz are shown for the 1980 May 9 and 1981 February 26 flares respectively. This frequency, which was used for the microwave source volume calculation discussed in this section, is in the optically thick part of the spectrum for both flares. The relative amplitudes of the different impulsive spikes in the hard X-ray emissions are quite different from those of the microwave emission for the time histories shown in Figures 2 and 3. For each individual spike, however, the rise time, fall time, and time of maximum are quite similar. The differences between the relative amplitudes of the emission peaks seen in the two wavelength ranges may be attributable to differences in the initial conditions in different parts of the flare, or possibly to a partial occlusion of the microwave emitting region by other nonflaring plasma.

It is generally accepted that the microwave emission is due predominantly to gyrosynchrotron emission from electrons confined within the flaring magnetic loop, while the hard X rays are due to bremsstrahlung of energetic electrons. It is not clear, however, whether the bremsstrahlung originates from a thermal source in which the electrons interact with their own plasma, or if it is due to the interaction of a beam of electrons impinging on a target of ambient solar medium. In the following, both thermal and nonthermal analyses are considered in an attempt to estimate the microwave source area and volume.

2.1.1 Thermal Analysis

In this approach, the effective temperature and emission measure of the X-ray source were determined under the assumption that the hard X rays were produced by bremsstrahlung radiation from thermal plasma which was optically thin with respect to the hard X rays. A statistical analysis of the observed X-ray spectra was carried out using the HXRBS data analysis procedures described by Dennis (1982) "HXRBS Spectral Analysis"

1980 May 9

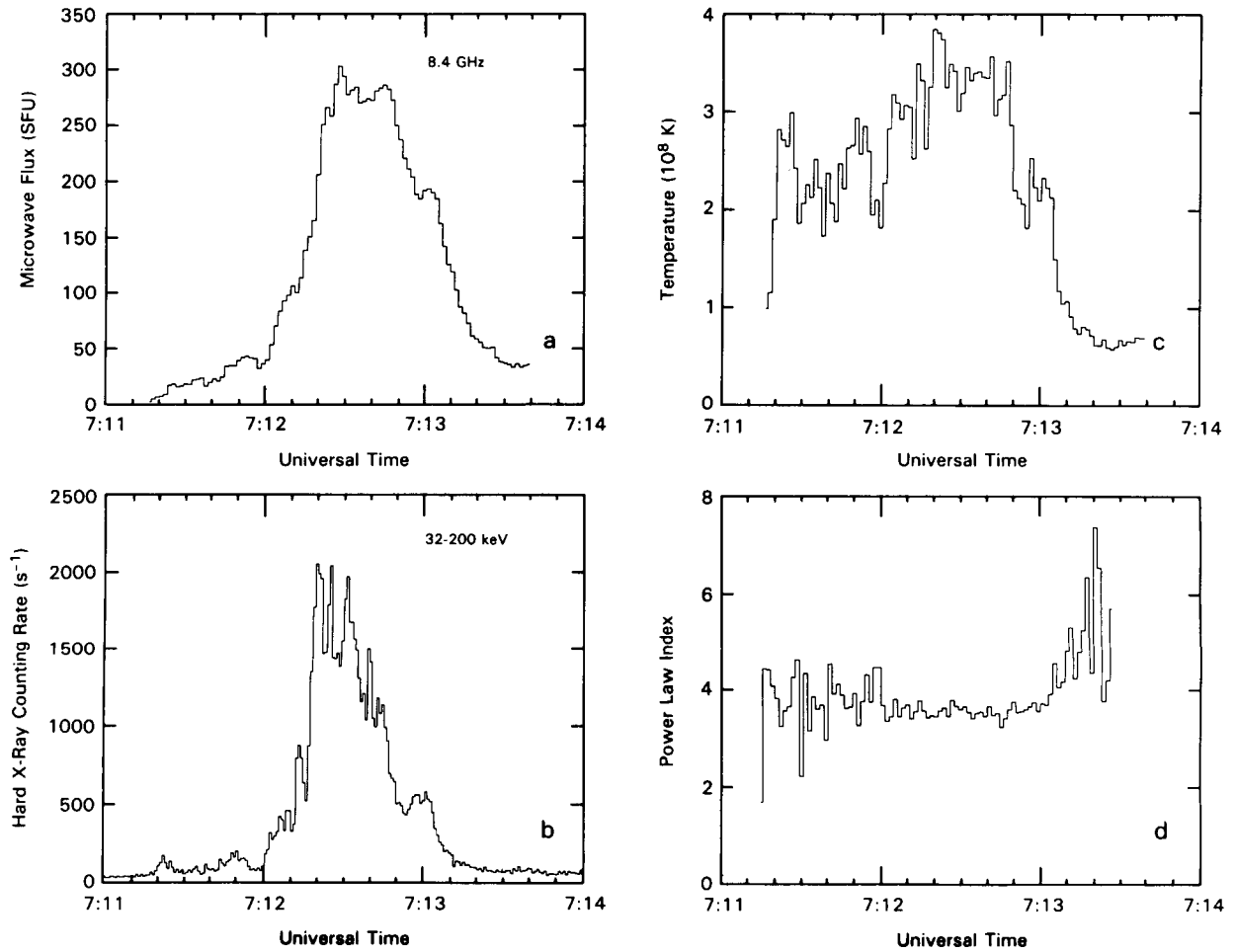


Figure 2. Time histories of various parameters during the 1980 May 9 flare. (a) Microwave flux at 8.4 GHz. (b) Hard X-ray counting rate, corresponding to the energy range from 32 to 200 keV. (c) Electron temperature inferred from the spectral analysis of the hard X rays, assuming a thermal energy distribution for the hard X-ray source. (d) Power-law spectral index of the source electron population, inferred from the spectral analysis of the hard X rays assuming a non-thermal source.

1981 February 26

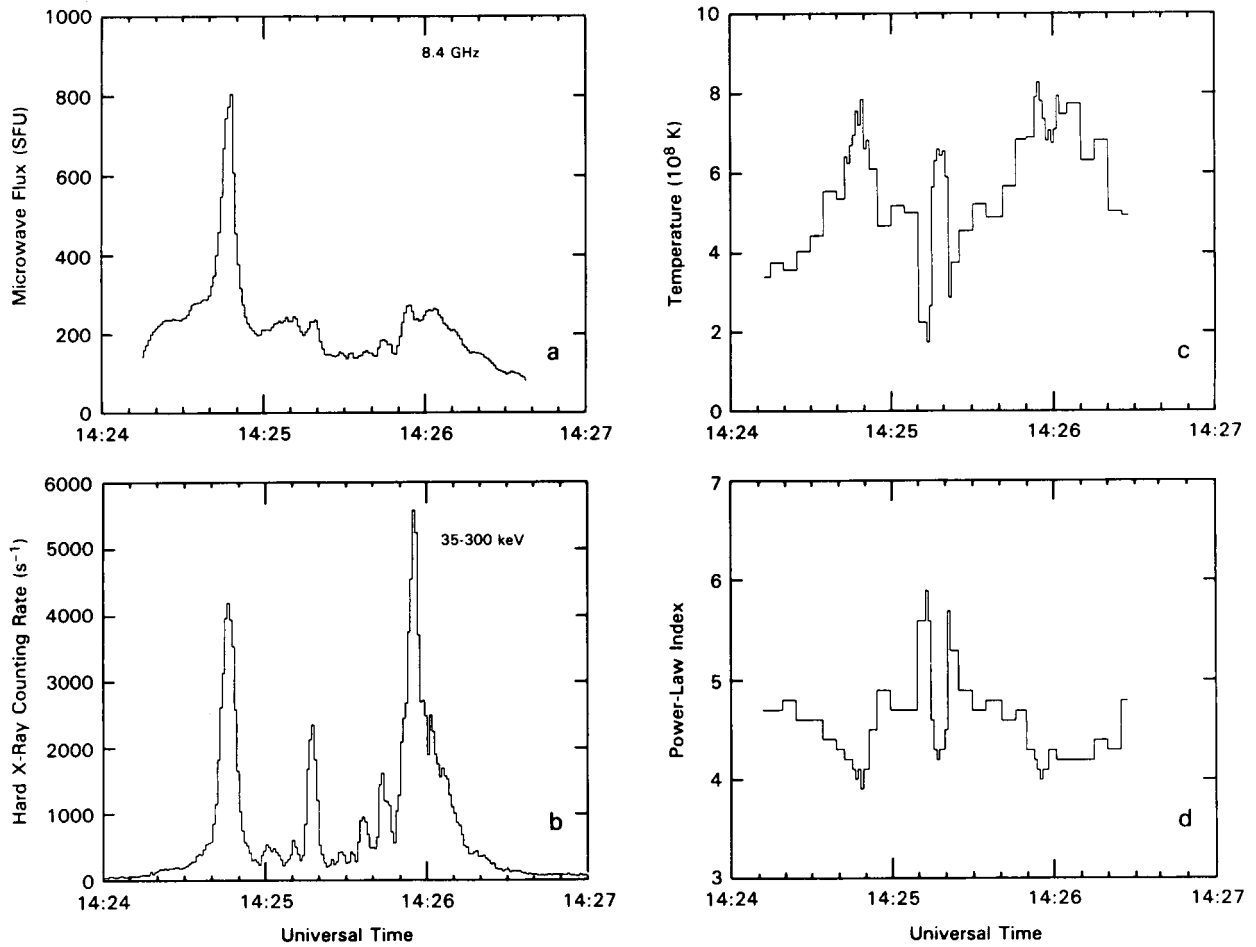


Figure 3. Time histories of various parameters during the 1981 February 26 flare. (a) Microwave flux at 8.4 GHz. (b) Hard X-ray counting rate, corresponding to the energy range from 35 to 300 keV. (c) Electron temperature inferred from the spectral analysis of the hard X rays, assuming a thermal energy distribution for the hard X-ray source. (d) Power-law spectral index of the source electron population, inferred from the spectral analysis of the hard X rays assuming a non-thermal source.

(unpublished technical report). This technical report is based on publications by Hoyng, Brown, and Van Beek (1976), Lin and Hudson (1976), and Brown (1971). The spectral form assumed for these calculations is:

$$\frac{dN}{dE} = CE^{1.4} \exp\left(\frac{-(E - E_m)}{kT}\right) \quad \text{photons cm}^{-2} \text{ s}^{-1} \text{ keV}^{-1}, \quad (1)$$

where E is the photon energy, dN is the number of photons with energy between E and $E + dE$, T is the temperature of the hard X-ray source, and k is the Boltzmann constant. The parameters C and T were determined by minimizing the chi-square obtained from the data and the expression given above. In this analysis, E_m was set equal to 50 keV, a "mean" energy of the range covered by the data. E_m is chosen in order to minimize the interdependence of the parameters C and T in the least-squares fitting procedure. C depends on the emission measure EM and the temperature T :

$$C = \frac{1.3 \times 10^{42}(EM)}{(kT)^{0.1}} \exp(-E_m/kT) \quad \text{cm}^{-3}. \quad (2)$$

From the observations of the flares studied here, it was possible to determine the shape and evolution of the microwave spectra throughout each event. Only the spectra corresponding to the flare of 1980 April 8 have a simple behavior; these show a simple rise and fall structure with the maximum close to 6 GHz. This turnover frequency remains constant, at least to within the spectral resolution of the observations. On the rising portion of the spectrum, the flux is approximately proportional to the square of the frequency. In the case of the 1980 May 9 and 1981 February 26 flares, the microwave spectra have complex shapes that change with time. During at least the first impulsive part of these flares, however, the spectra also show a simple rise and fall, with the maximum intensity at about 10 GHz. Throughout the remainder of each flare, a relative maximum or an inflection point is visible at the same frequency. If the source of radiation is optically thick and homogeneous, the microwave spectrum below the turnover frequency is described by the Rayleigh-Jeans law. For a source at a distance of one AU, the flux can be expressed as:

$$S(f) = 0.16 A_{eff} f^2 kT \quad \text{SFU}, \quad (3)$$

where S is the microwave flux in SFU , ($1 SFU = 10^{-22} W m^{-2} Hz^{-1}$), f is the frequency in GHz , kT is the source temperature in keV , and A_{eff} is the effective area of the microwave source in units of $10^{18} cm^2$ (Crannell *et al.*, 1978). For frequencies above the turnover frequency, the radiation becomes optically thin and the spectrum falls with a spectral index of about seven (Mätzler, 1978) in the case of gyrosynchrotron emission. Deviations from this behavior in the optically thin part of the spectrum, and from the Rayleigh-Jeans law in the optically thick part, are to be expected, however, if the microwave source is inhomogeneous. In this analysis, the temperature is derived from the hard X-ray observations. The area of the source can then be inferred from the measured microwave flux. The volume of the source is estimated by raising A_{eff} to the power $3/2$.

The common temperature assumption does not necessarily imply that the sources of microwaves and hard X rays are identical. For example, the microwaves might originate from a population of energetic electrons located near the top of the flaring magnetic loop, while the hard X rays result from bremsstrahlung emission as part or all of the electrons move to denser regions at the loop footpoints. The assumption would be only approximately true if the electron population were multi-thermal, or if the higher energy electrons escape preferentially to the loop footpoints.

There are three possible sources of error in this method of inferring the microwave source area and volume from the Rayleigh Jeans law. First, the area inferred this way corresponds only to that part of the microwave source, which is optically thick to radiation below the turnover frequency. It therefore represents a lower limit on the total effective area of the whole microwave source which also comprises regions that are optically thin to microwave radiation. Secondly, inhomogeneities within the microwave source can cause a frequency dependence of the calculated area, thereby also causing deviations from the Rayleigh-Jeans law. (Schoechlin and Magun, 1979). This effect was investigated for all three flares, and was found to be important in the case of the 1980 May 9 and February 26 events. In these cases, the areas inferred from the microwave flux at $5.2 GHz$ were found to be greater by a factor that varied from 1 to 3 than the areas corresponding to $8.4 GHz$ from which we calculated the source volumes presented in this study. A third source of uncertainty is introduced by our procedure of esti-

mating the volume as $(A_{eff})^{3/2}$. This uncertainty can be evaluated for other assumed geometries for the source of microwaves. For a loop with aspect ratio r , which is the ratio of the loop length to the loop width, $(A_{eff})^{3/2}$ is larger than the true volume by the factor $F = 0.65r^{0.5}$ if the loop is seen from above. If the loop is seen in profile, the factor is $F = 4/\pi r^{0.5}$. Typical values of the aspect ratio are of order 10 (Colgate, 1978, Van Hoven, 1981, Batchelor *et al.*, 1985), suggesting that $(A_{eff})^{3/2}$ is an overestimate of the true source volume by a factor that is probably no greater than 4.

2.1.2 Non-Thermal Analysis

In this approach, the hard X rays are assumed to be produced by bremsstrahlung of energetic electrons incident on the ambient solar medium, and characterized by a power-law distribution in energy. The photon spectrum is of the form (Dennis, 1982):

$$\frac{dN}{dE} = A_1(E/E_m)^{-A_2}, \quad (4)$$

where E is the photon energy in keV, and the parameters A_1 and A_2 are determined by a statistical analysis of the data. As for the spectral analysis assuming a thermal source of hard X rays, E_m is chosen to be 50 keV in order to minimize the interdependence between A_1 and A_2 during the least-squares fitting procedure.

If the beam of electrons is incident on a region of high density where it loses all its energy on a very short time scale, then a continuous flux of electrons injected in the hard X-ray source is necessary to produce the observed photon spectrum. In this case of "thick target emission", the electron flux is related to the photon spectrum according to the following expressions (Dennis, 1982):

$$\begin{aligned} I(E) &= B_1 E^{-B_2} \quad \text{electrons } keV^{-1}, & (5) \\ B_1 &= 3 \times 10^{33} A_1 E_m^{A_2} A_2 (A_2 - 1)^2 b(A_2 - \frac{1}{2}, \frac{1}{2}), \text{ and} \\ B_2 &= A_2 + 1, \end{aligned}$$

where b is the beta function. The electron population power index, obtained from the spectral analysis of the hard X rays assuming thick target emission, is plotted as function of time in Figures 2 and 3 for the 1980 May 9 and 1981 February 26 flares respectively.

The optically thick part of a microwave spectrum produced by non-thermal electrons also can be parameterized by the Rayleigh-Jeans law, as in the thermal case, but using an effective temperature T_{eff} (Dulk and Marsh, 1982). This effective temperature also depends on B_2 , the power-law spectral index of the electron population, on θ , the viewing angle between the line of sight and the magnetic field lines, and on the ratio of the microwave frequency to the gyrofrequency f_B :

$$T_{eff} = 2.2 \times 10^9 - 0.31B_2 (\sin \theta)^{-0.36 - 0.06B_2} \left(\frac{f}{f_B} \right)^{0.50 + 0.085B_2} \quad (6)$$

In our analysis, we calculated the effective temperature using the power index obtained from the thick-target spectral analysis of the hard X rays. We also assumed a viewing angle of 45 degrees and a typical magnetic field of 300 Gauss (gyrofrequency equal to 0.84 GHz). This was done following the study of Gary (1985). In six of the eight flares he examined, Gary found that under these assumptions and the assumption that the microwave source is homogeneous, the calculated number of electrons emitting microwaves is in close agreement with the calculated number of electrons emitting hard X rays.

Following the same method described in Section 2.1.1, the effective area and volume of the microwave source was calculated using the flux measured at 8.4 GHz.

2.2 The Soft X-ray Analysis

High resolution X-ray spectra were obtained during the three flares with the SOLEX-B Bragg crystal spectrometer aboard the *P78-1* satellite. The resonance $1s^2 \ ^1S - 1s2p \ ^1P$ (21.602 Å), intercombination $1s^2 \ ^1S - 1s2p \ ^3P_{1,2}$ (21.804 Å), and forbidden $1s^2 \ ^1S - 1s2s \ ^3S$ (22.097 Å) lines of

the helium-like O VII ion were measured, thus enabling a determination of the electron density and emission measure of the 2×10^6 K soft X-ray source. For plasma of this temperature, the volume is obtained by dividing the emission measure by the square of the electron density. The determination of these parameters rests on the assumption that the source was small compared to the one-arc-minute SOLEX-B field of view and was centered in that field of view. The use of these assumptions is believed to result in an underestimate of the volume by less than a factor of two. The soft X rays were analyzed by making use of theoretical calculations and a refinement of the SOLEX response function that have become available since the publication of the article by Doschek *et al.* (1981), in which the flares of 1980 April 8 and 1980 May 9 were discussed. The new results differ somewhat from those of the earlier article. The determination of the O VII temperature from the G ratio of the forbidden plus intercombination to the resonance line flux was based on theoretical data of Pradhan (1982) and Keenan, Tayal, and Kingston (1984) and laboratory measurements by TFR Group, Doyle, and Schwob (1982). For the 1980 May 9 event, G was found to be 0.80, corresponding to a temperature of 2.5×10^6 K. During the 1981 February 26 event, G varied between 0.9 and 1.3, and a temperature of 2.0×10^6 K was used for the analysis. In all cases, the statistical uncertainty on G for a single measurement was typically 0.1.

The temperature affects the formula for obtaining the electron density n from the R ratio of the forbidden line flux to the intercombination line flux. The expressions for electron density are based on the work of Keenan, Tayal, and Kingston (1984):

$$n = 3.1 \times 10^{10} \left(\frac{3.95}{R} - 1 \right) \quad (7)$$

for the 1980 May 9 event, and

$$n = 3.1 \times 10^{10} \left(\frac{3.90}{R} - 1 \right) \quad (8)$$

for the 1981 February 26 event. The emission measure of the soft X-ray source was calculated by using the resonance line emissivity at the corresponding temperatures, determined from calculations by W. D. Robb that were parameterized by Magee *et al.* (1977).

The densities obtained from Equations (7) and (8) were compared to estimates of the electron density based on calculations by Bely-Dubau, Faucher, and Gabriel (private communication, March 1987). The latter estimates were systematically greater than the densities obtained from the equations above by a constant factor during each flare. This factor was found to be 1.41 for the April 8 and February 26 flares, and 1.44 for the May 9 flare. These uncertainties in the determination of the electron density are less significant than the uncertainty arising from the background emission discussed below.

An important question regarding both the analysis and the interpretation of the results is whether or not the preflare O VII line emission should be treated as background. The observations themselves provide no means for distinguishing between two extreme possibilities, so the data were analyzed to determine the implications of both extremes. One of the possibilities is that the flare took place against an unchanging background of active-region emission, with a constant spectrum represented by the preflare measurements. For this case, the line fluxes from the preflare emission were subtracted from the total flux measured during the flare before the R and the G ratios were calculated. For the 1980 May 9 event, the R ratio calculated from the background spectrum was $R = 2.43 \pm 0.6$ which is indicative of a high density rarely observed in a nonflaring region ($2 \times 10^{10} \text{ cm}^{-3}$). It is not known whether this emission arose from a flare precursor or from a general active-region background. The other extreme is that the flare disrupted the source region from which the preflare emission arose so that the preflare emission did not persist throughout the flare. A second analysis was therefore carried out in which no subtraction of preflare line fluxes was performed. In both cases, of course, the background continuum measured with each spectrum was subtracted before the line fluxes were determined.

3 RESULTS

3.1 Results From the 1980 April 8 Flare

Figure 4a illustrates the volumes calculated for the impulsive and gradual sources that produced the 1980 April 8 event. The curve representing the thermal microwave source volume was not recalculated in the present work, but is taken from Chapter 5 of the *SMM* Workshop proceedings (Wu *et al.*, 1986). The hard X-ray and microwave observations that were reported at the workshop have been reanalyzed here in order to obtain volume estimates based on the nonthermal approach, as well. The results from the two analyses are essentially the same. In both cases, the impulsive microwave source volume expands very rapidly at the beginning of the flare, and reaches a maximum value of $2 \times 10^{28} \text{ cm}^3$ corresponding to an angular extension of about 40 *arcseconds*. The second maximum of the microwave source volume which occurs at 03:11:00 UT is real, even though it does not appear clearly in the results of the nonthermal volume calculation. It is interpreted as being due to another source of radiation flaring in the same active region. As discussed below, this interpretation is supported by imaging observations of this event obtained with the Hard X-Ray Imaging Spectrometer (HXIS) and with the Flat Crystal Spectrometer (FCS) on board the *SMM* satellite.

In Figure 4a, the volume inferred from the O VII line emission is also plotted as a function of time. The points indicated by diamonds and crosses are the results of analyses done with and without the preflare line intensity subtraction, respectively. The same conventions hold for Figure 4b showing the electron density inferred for the O VII source. The error bars on each point indicate only the statistical uncertainties. The time required to scan the O VII line region was 7.62s during these observations. The HXIS observations of this flare indicate that this was a complex event with more than one source of radiation. At the *SMM* Workshop, a “kernels plus tongue” structure was reported for this flare, such as that described by Orwig *et al.* (1981) and by van Beek *et al.* (1981) in the case of the limb flare of 1980 April 30. During the April 8 event, the light curves (3.5 to 8.0 keV) of two sources situated roughly 100 *arcseconds* apart reach their

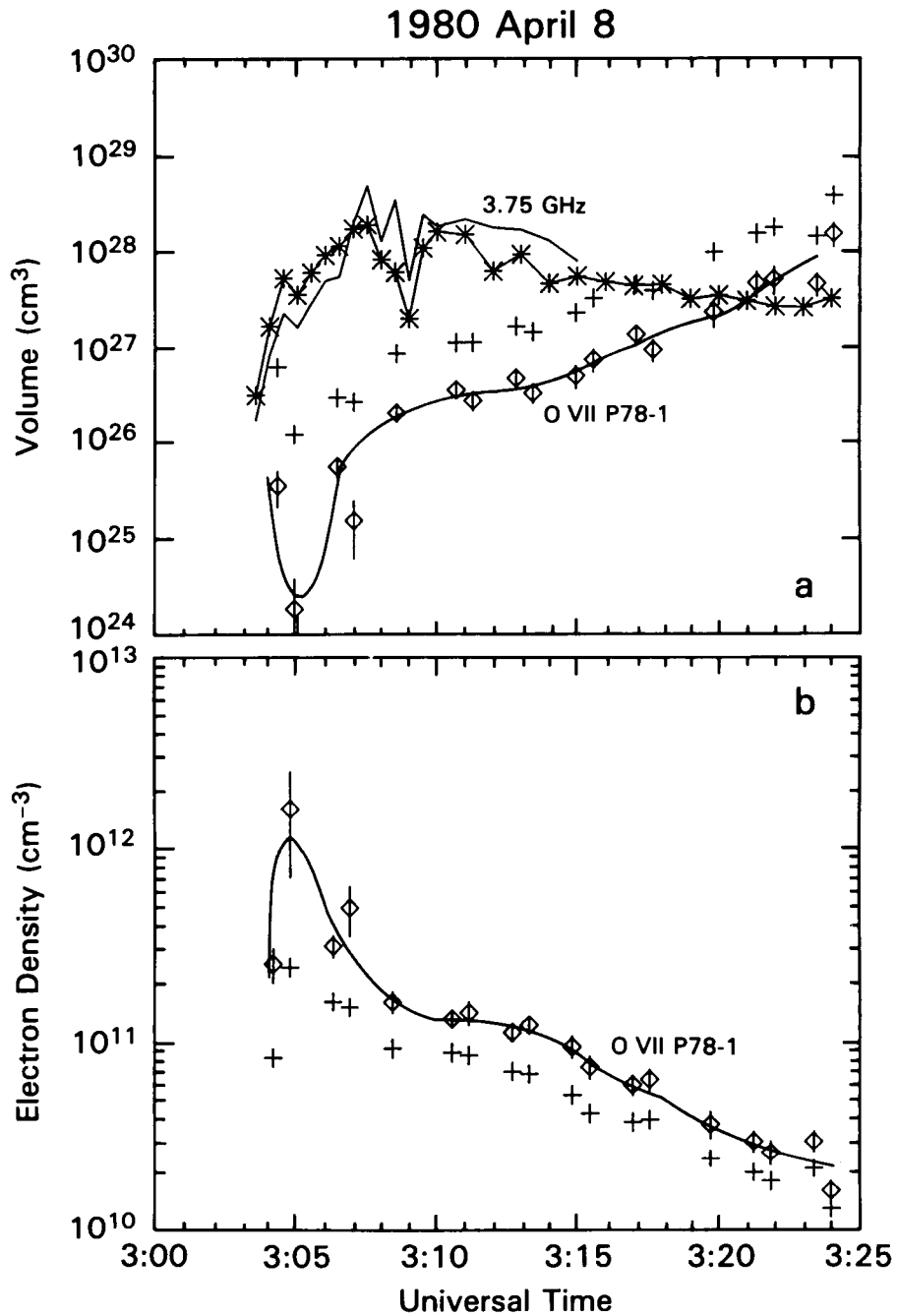


Figure 4. For the 1980 April 8 flare, results of the source volume and density calculations as functions of time. (a) A comparison of the microwave/hard X-ray volume to the soft X-ray volume for the 1980 April 8 flare. The asterisks represent the volume of the microwave/hard X-ray source obtained from a thermal analysis of the hard X-ray spectrum. The other line (without asterisks) gives the volume calculated from a non-thermal analysis of the hard X-ray spectrum. The error bars without diamonds show the O VII source volume, calculated without subtraction of the preflare line fluxes. Error bars with diamonds show the O VII volume, calculated with preflare line fluxes subtracted out. The curve through the error bars with diamonds is not the result of a calculation and is drawn only to guide the eye. (b) Electron density of the soft X-ray source, calculated from the O VII line emission. The symbol convention is the same as in Figure 4a. The line through the error bars with diamonds is not the result of a calculation and is drawn only to guide the eye.

peak intensities at 03:07:00 UT and at 03:11:00 UT, which are also the times of the maxima of the microwave source volume plotted in Figure 4. From their analysis of the HXIS observations, and from the neutral line configuration that they deduce from MSFC magnetograms, Machado *et al.* (1983) also infer a complex geometry for the magnetic field in the active region during this event. While the details of the source geometry are not critical for the present work, the complexity precludes any interpretation of the dynamics that involves only a single loop.

The FCS data that we analyzed for this event consist of a sequence of raster images obtained throughout the event with each of the six FCS detectors. Thus, sequences of images were obtained in emission lines from O VIII, Ne IX, Mg XI, Si XIII, S XV, and Fe XXV. Each raster image consists of an array of 16 by 16 pixels. The spatial resolution of one image is determined by the angular step size of 15 *arcseconds* and the temporal resolution, by the integration time of 1.024 s per pixel. These images also reveal that there were two sources of soft X rays during the flare, situated five or six pixels apart in the East-West direction. The larger source, which was the first to reach its maximum intensity at the beginning of the flare, is spatially resolved on the images obtained in O VIII, Ne IX, Mg XI and Si XIII. After these observations were deconvolved with the instrumental response function, it was possible to measure the effective area of the source at different temperatures as it appeared between 03:08:15 UT and 03:12:41 UT. The results are illustrated in Figure 5. In the images obtained with the higher temperature channels, the two sources appear closer together, and are merged at half maximum. Indeed, according to Machado *et al.* (1983) the geometry is quite complicated. The curve in Figure 5 shows a very steep temperature dependence of the apparent area, for temperatures lower than 10^7 K. An extrapolation of this curve down to 2×10^6 K, which is the temperature of the O VII line emission, is dubious. Only a lower limit of 4×10^{18} cm² can be given for the effective area of the O VII source. An upper limit to the source thickness can be estimated from this area and from the volume that was found to be approximately constant during this period of time. Assuming a filling factor of unity, we found an equivalent thickness of approximately 800 km for the O VII source between 03:08 and 03:12 UT.

1980 April 8

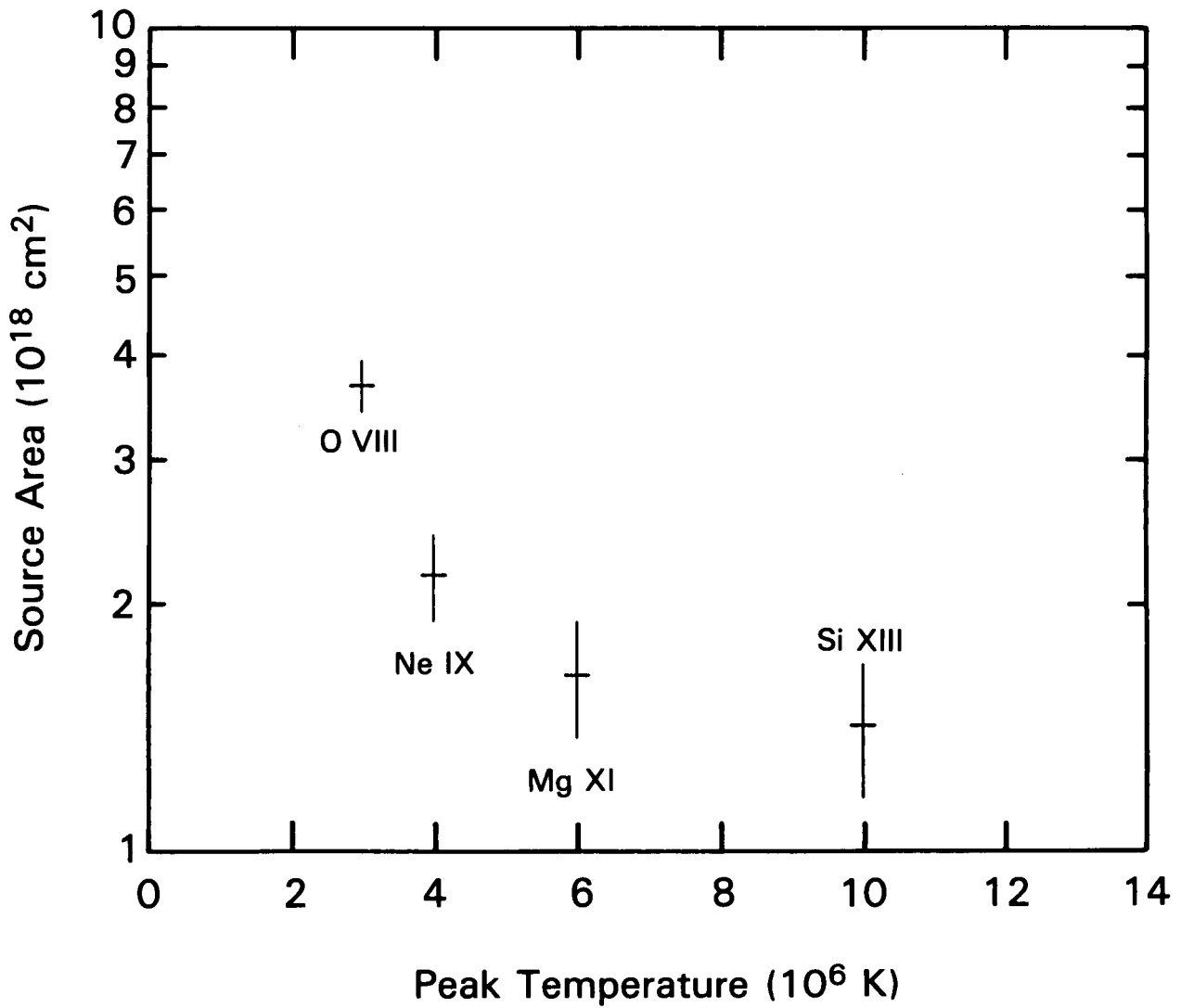


Figure 5. For the 1980 April 8 event, source areas of the soft X-ray line emission are plotted as a function of the corresponding peak temperature. These areas correspond to the larger and more westerly of the two sources of radiation during this flare. The time interval is 03:08:15-03:12:41 UT. The areas were inferred from the XRP/FCS raster images, after deconvolving the data with the instrumental response function, and taking a full width half maximum criterion.

3.2 Results From the 1980 May 9 Flare

The microwave source volume is plotted as a function of time in Figure 6 for the 1980 May 9 flare. For this event also, the results obtained from the thermal analysis are very similar in their temporal behavior to those obtained from the nonthermal analysis, with the assumed values of 45 degrees for the viewing angle and 300 Gauss for the magnetic field. The thermal volume is greater than the nonthermal volume by about a factor of three, which could be accounted for by other choices of the angle and field. Both curves in Figure 6 have the same trend, with an impulsive rise followed by a more gradual decrease after the peak of the emission.

Figure 7a and Figure 7b show the results of the analysis of the O VII emission. Here also, the error bars on the volumes and densities reflect only the statistical uncertainties. The time required to complete one scan of the O VII line complex was 7.62 s. Although the sampling intervals are spaced apart by several tens of seconds, it is apparent that the O VII source volume is at its minimum at nearly the same time as when the microwave source volume first reaches its maximum. This is also the time when the electron density inferred from the O VII lines is the greatest. In the results of the analysis done with the preflare spectrum subtraction, it is not clear whether the volume initially decreases or the volume starts out small and steadily increases, because of the large uncertainties in the first two density measurements.

The HXIS observations of this flare, which were discussed also by Machado (1983), indicate that this was a compact event. There was only one source of X rays in the active region, and its extension was a little less than 30 arcseconds. This is comparable to our estimate of the microwave source size. Assuming a one loop geometry for the source, with an aspect ratio of 1/10 and an apparent area equal to $1 \times 10^{18} \text{ cm}^2$, one would expect a distance of 33 arcseconds between the footpoints, if the loop were seen from above.

1980 May 9

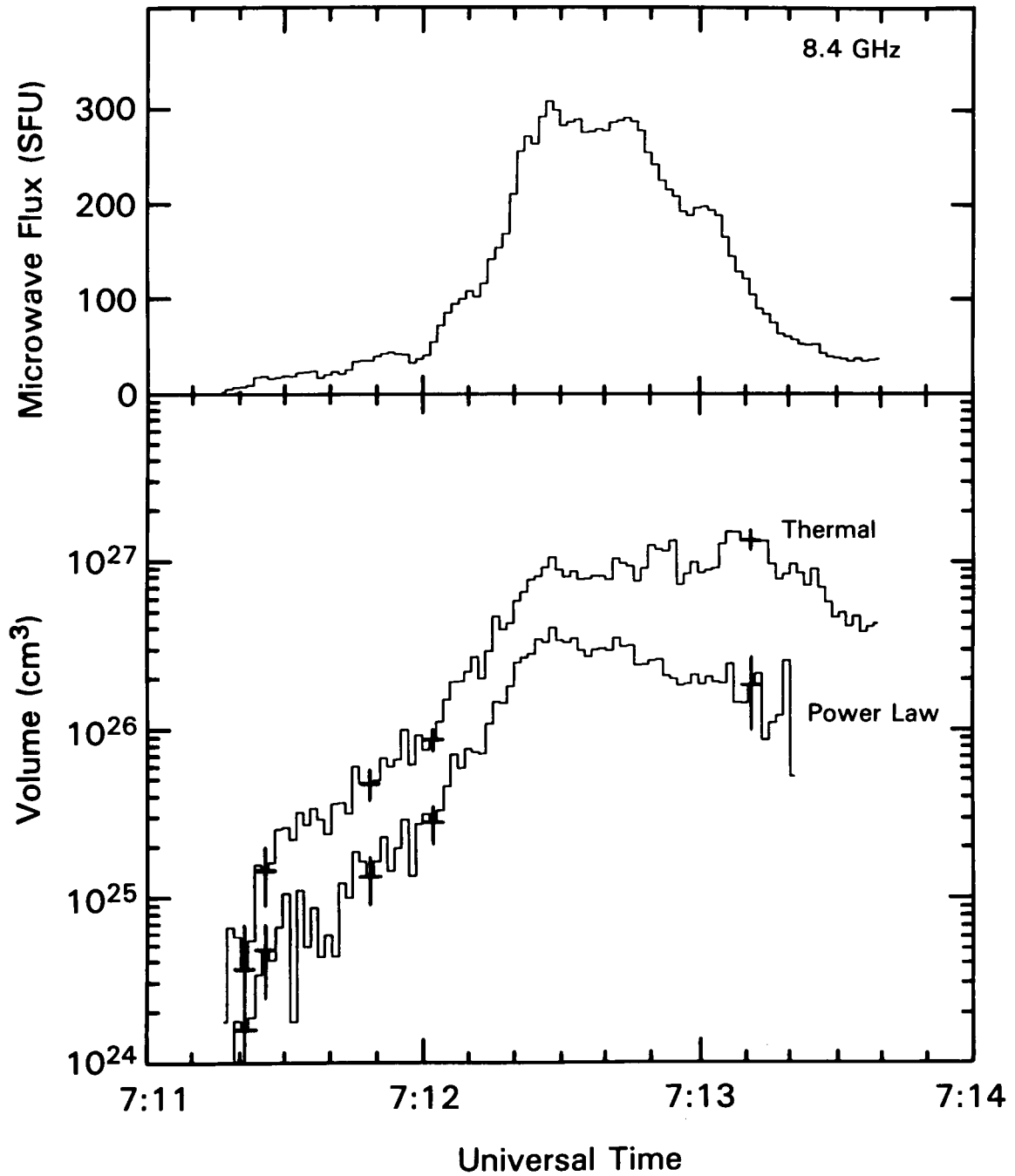


Figure 6. Flare volumes for the 1980 May 9 event, calculated from the microwave emission (8.4 GHz) and the hard X-ray spectral analysis. The 8.4 GHz microwave time history is also plotted across the top of the page for comparison. The upper curve in the bottom panel represents the volume derived under the assumption that the hard X rays were emitted by a hot thermal plasma. The bottom curve represents the volume derived under the assumption that the hard X-ray emission arose from a non-thermal population of electrons incident on a thick target. The error bars reflect only the statistical uncertainties.

1980 May 9

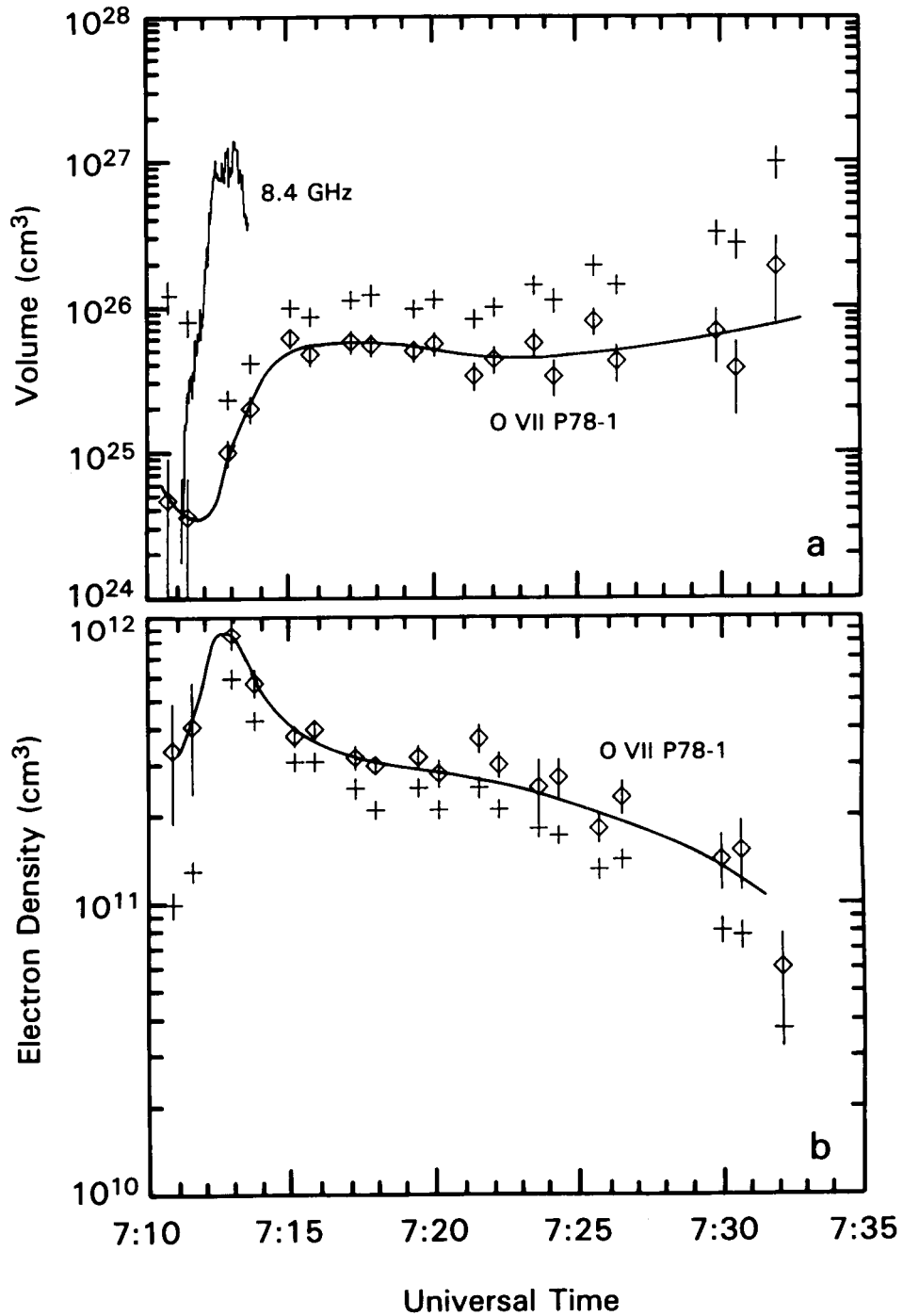


Figure 7. Results of the O VII line analysis for the 1980 May 9 event. (a) Comparison of the microwave/hard X-ray volume and the soft X-ray volume with the same format as in Figure 4. Again the error bars with diamonds represent the results obtained when preflare line fluxes are subtracted before the analysis is performed. (b) Electron density of the soft X-ray source, calculated from the O VII line emission. The format is the same as that of Figure 4.

3.3 Results From the 1981 February 26 Flare

In Figure 8, the volumes obtained from the hard X-ray and microwave analyses are plotted as functions of time for the flare of 1981 February 26. The two curves represent the results of the calculations based on the thermal and on the power-law, thick-target spectral analysis of the hard X rays. Both calculations predict essentially the same results, with a systematic difference that may be accounted for by the choice of the magnetic field and viewing angle in the nonthermal model calculation. It must be emphasized that this was a complex flare and the results of this estimate of the microwave source volume are not reliable after the first impulsive peak of microwave emission. After this time the optical thickness of the microwave spectrum at 8.4 GHz is questionable, and during each of the peaks in the hard X-ray time history, the X-ray spectra are better represented by double power-law emission rather than by single temperature or power-law spectra. During the rising phase of the microwave emission, between 14:24:15 UT and about 14:24:40 UT, the thermal volume increases sharply to a value of $4.5 \times 10^{26} \text{ cm}^3$ which corresponds to a characteristic dimension of about 7700 km or 10 arcseconds. This is a typical size for a flaring loop which extends from the chromosphere into the corona. The spike in the volume at 14:24:48 UT corresponds to the sharp peak in the microwave time history, also shown in Figure 8 for comparison. At the time of this spike, a significant change in the polarization of the microwaves was observed. This suggests that the sudden increase in the volume was due to another source flaring briefly after the onset of the first, longer-lived source of radiation. The peaks that appear both in the thermal and in the nonthermal volume curves between 14:25:00 UT and 14:25:30 UT do not correspond to a change in intensity or polarization of the microwaves, but are due to sharp changes in the hard X-ray spectrum just before and after the peak in the hard X-ray emission at 14:25:18 UT.

Figures 9a and 9b illustrate the results of the O VII source volume calculations obtained with and those obtained without the preflare spectrum subtraction described in Section 2.2. The O VII line emission remained intense enough to allow determination of density and emission measure until almost ten minutes after the end of the hard X-ray and microwave emission. The gap in the O VII data between 14:25:00 UT and

1981 February 26

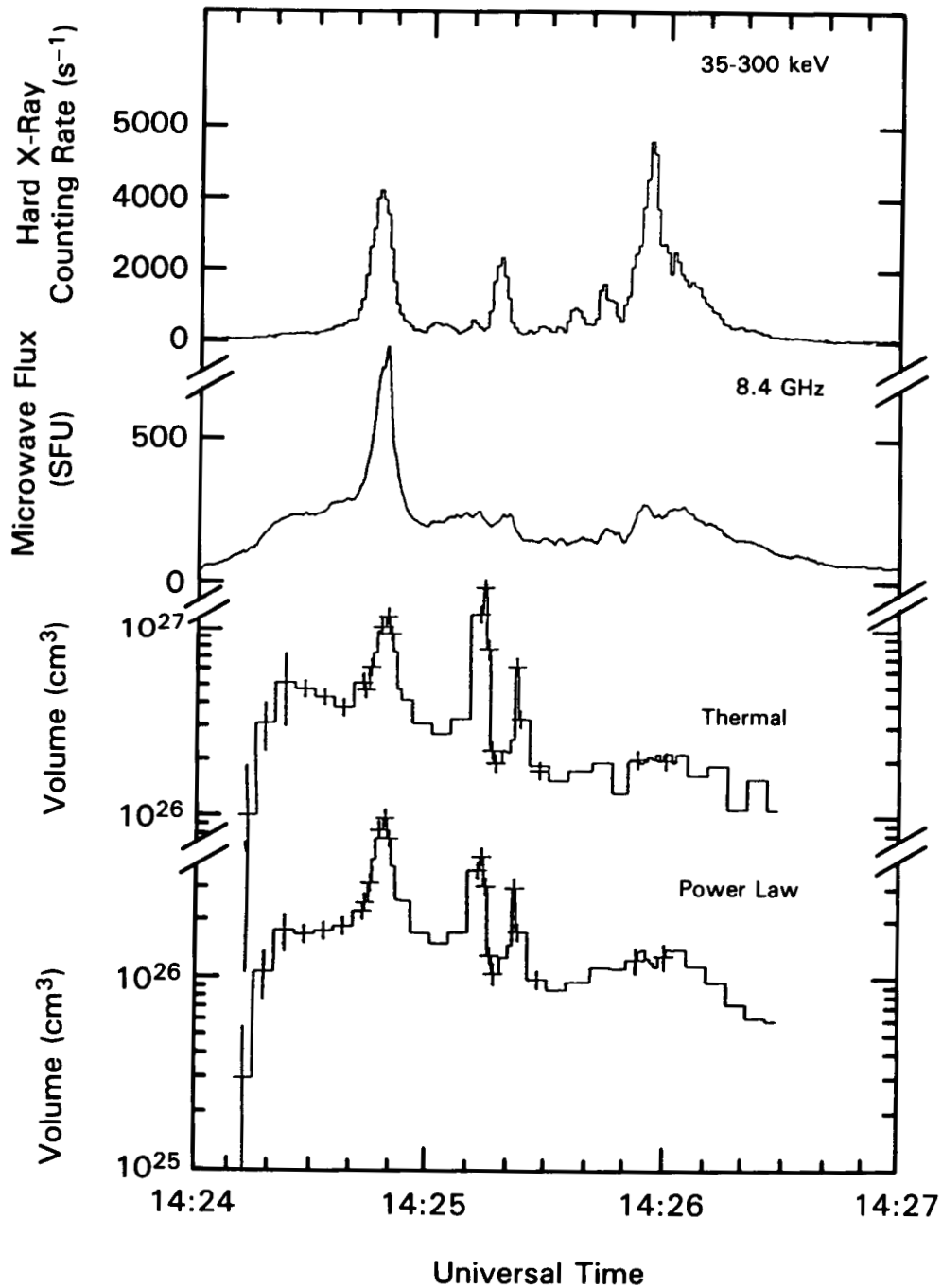


Figure 8. For the 1981 February 26 event, the flare volume calculated from the 8.4 GHz microwave emission and the spectral analysis of the hard X rays. The 8.4 GHz microwave time history and the hard X-ray counting rate are also plotted for comparison. The upper curve in the bottom panel represents the volume derived under the assumption that the hard X rays were emitted by a thermal plasma. The bottom curve represents the volume derived under the assumption that the hard X-ray emission arose from a non-thermal population of electrons incident on a thick target. The error bars reflect only the statistical uncertainties.

1981 February 26

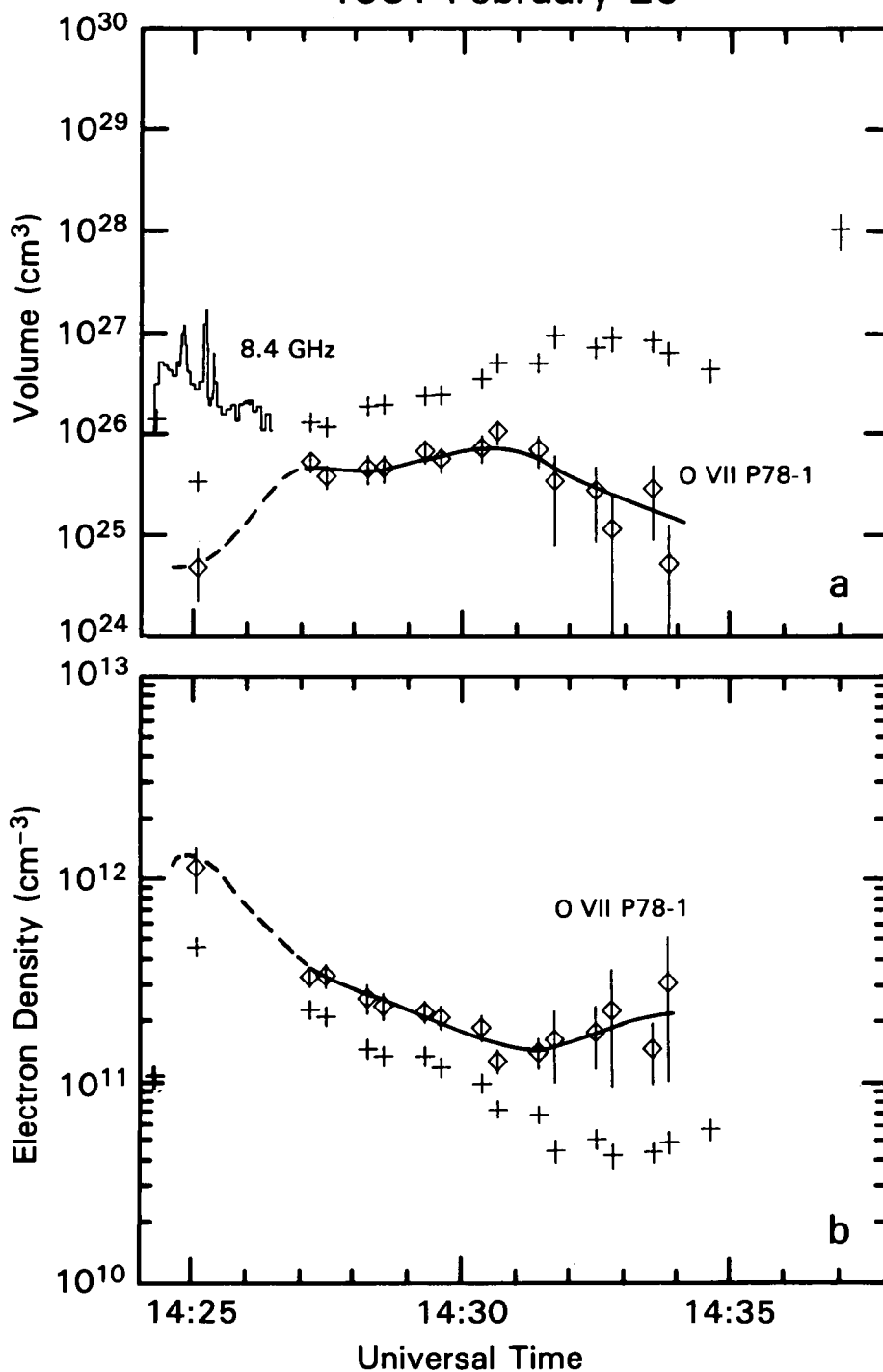


Figure 9. Results of the O VII line analysis for the 1981 February 26 event. (a) Comparison between the microwave/hard X-ray and the soft X-ray volumes, using the same format as in Figure 4. The error bars with diamonds represent the results obtained when preflare line fluxes are subtracted before the analysis is performed. (b) Electron density of the soft X-ray source, calculated from the O VII line emission. The format is the same as that of Figure 4.

14:27:00 UT occurred because the *P78-1* pointed instrument assembly, on which the SOLEX spectrometers were mounted, pointed at Sun center for a white light coronagraph exposure. Unfortunately, the gap occurred at the time of the peaks in the hard X-ray and microwave emission so that it is not possible to say precisely when the O VII source density was at its maximum, nor when the source volume was at its minimum. The error bars on the volume and density plots represent uncertainties due to counting statistics, only. The times that are indicated correspond to when the spectrometer was scanning the center of the O VII complex. For this flare, the time required for each scan was 3.81 s.

4 DISCUSSION

The flares studied here differ greatly in their sizes and spectral parameters. They also differ in the time-intensity profiles of their impulsive emissions. The volumes derived from these observations, however, show striking similarities in temporal evolution. For two of the three events, the microwave source exhibits first an impulsive expansion followed by a more gradual decrease. Also, in each case, the expansion terminates at approximately the time of peak impulsive emission. In the case of the 1980 April 8 and May 9 flares, the volume of the soft X-ray emission exhibits an increase that begins approximately at the impulsive emission peak. This cannot be asserted in the case of the 1981 February 26 event because of the gap in the soft X-ray observations at the beginning of the flare. The corresponding soft X-ray density declines as the volume increases.

In order to calculate volumes of the microwave sources, we assumed that the spectrum of the electron population responsible for these emissions could be well represented by the spectrum of the electrons responsible for the associated hard X-ray emissions. While it is not necessary for a hard X-ray source to be in the same location as its associated microwave source, the energizing mechanisms for the two sources must be related for the required assumption of common spectrum to be physically reasonable. This distinction is particularly important when the data are interpreted in the context of a physical model such as the following.

The observed rise in microwave source volume is consistent with the results of Starr *et al.* (1987), who interpreted it in terms of a collisionless conduction front model. In the context of this model, a front travels from the apex to the footpoint of a loop, sweeping out an increasing source volume for all impulsive emissions. The intensities of these emissions peak at or near the time when the front reaches the loop footpoint and their common source fills the loop. The detailed structures of the respective source volumes, however, are expected to be significantly different. All of the hard X-ray emission is optically thin and originates predominately from the highest density portions of the loop. The observations used to calculate the microwave volume, on the other hand, are explicitly chosen to be optically thick, and this emission originates predominately from regions

of the highest temperature and magnetic field strength, as well as density. In this, or in any model in which the source is the whole loop, the hard X-ray and microwave source volumes have a common origin, but their centers of density and detailed distributions might well be quite different. Each might effectively occupy only a fraction of the loop. An important implication for the interpretation of the present results is that the maximum microwave source area determined in the present analysis represents a lower limit on the actual projected area of the loop.

As suggested by the cartoons in Figure 10, the soft X-ray source volume starts out small near the beginning of the flare, then increases as the flare progresses. This appears in the results of analyses done with and without the preflare spectrum subtraction (shown schematically in the curves of Figure 10). The initial decrease in volume may be an observational artifact, because the decrease significantly diminishes when the preflare flux is subtracted. We attribute this apparent decrease to the brightening of a small source of soft X rays at the beginning of the flare rather than to a real contraction of the source volume. As a result of the heating by the overlying plasma (either by downstreaming electrons or by thermal conduction), the soft X-ray emission from the footpoints intensifies until they become the dominant sources within the field of view (phase II in Figure 10). The resulting average spectrum will change from one representing the general active-region background to one that characterizes the more intense sources at the footpoints. This, in turn, will cause an increase in the density derived from the O VII lines and a corresponding decrease in the apparent volume, relative to the initial values determined from the preflare spectra. Chromospheric evaporation then accounts for the ensuing expansion of the source (phase III in Figure 10), as suggested by the decrease in electron density averaged over the whole volume. The material ejected from the chromosphere in this way may then fill part of the microwave-source loop or another magnetic loop situated in the same active region, depending on the geometry of the magnetic field. The O VII emission reflects only that part of the volume which is in a temperature range of approximately $1-4 \times 10^6$ K. Once the O VII source has attained its maximum size, it is observed to remain constant for an interval of minutes (phase IV in Figure 10). After this "plateau phase", the emission measure and calculated

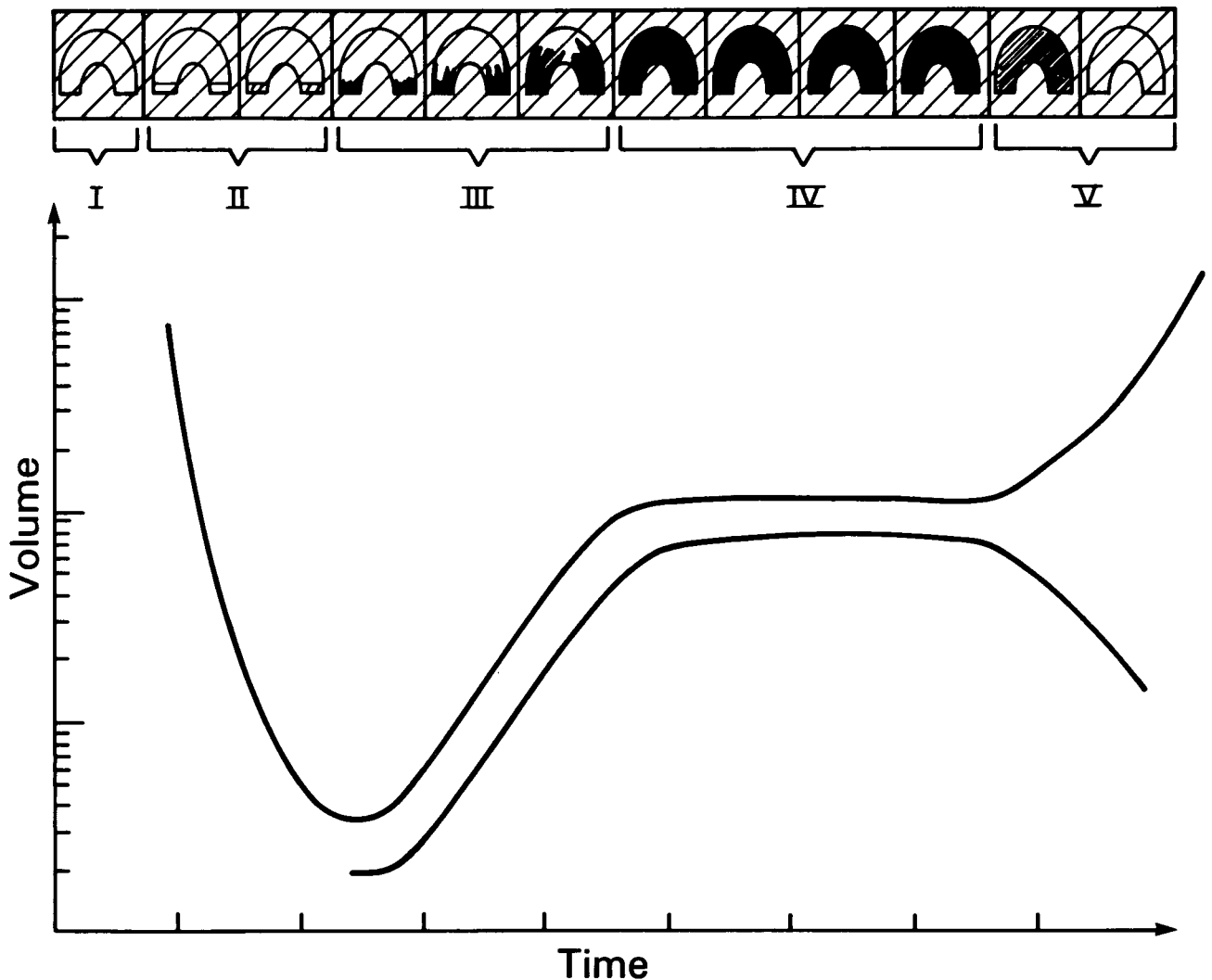


Figure 10. Diagram illustrating our interpretation of the results of the O VII source volume calculation. The cartoon at the top of the page represents the O VII source at successive times during the flare. The top and bottom curves represent schematically the results of the analysis done without and with the preflare spectrum subtraction, respectively. The initial and the final large values of the volume obtained without preflare line flux subtraction (top curve) are not real. They do not reflect a localized source, but result from the general active region emission as discussed in the text. The numerals under the cartoon indicate different stages of the O VII source volume calculation: PHASE I: Preflare situation: Background covers the whole field of view. PHASE II: Apparent decrease of the volume: Footpoints gradually dominating over the background within the field of view as a result of flare heating. PHASE III: Increase of the O VII source volume: Expansion resulting from chromospheric evaporation. PHASE IV: O VII source volume remains constant: The region emitting the O VII line has expanded to fill the portion of the loop system available to it as defined by the magnetic field configuration. PHASE V: The soft X-ray source fades away. The field of view is once again defined by the preflare background.

densities return to their preflare values, thus producing an apparent increase in volume at the end of the flare (phase V in Figure 10).

In the case of the 1980 April 8 flare, the plateau phase in the O VII volume lasts only for four or five minutes, then the volume expands again after approximately 03:12:00 UT. We attribute this increase to chromospheric evaporation taking place also in the other flaring source of radiation, observed in the same active region, and causing the second maximum in the microwave source volume.

The analysis of the O VII line emission with the preflare emission subtraction is based on the assumption that the preflare and postflare emission comes from a region that plays no real part in the flare. It originates from the active region within the field of view of the spectrometer, and is left unchanged by the event. The volumes and densities that are inferred from its spectrum do not correspond to a localized source. Alternatively, the expansion of the thermal plasma emitting soft X-rays may disrupt the region from which the preflare O VII emission arose. In this case it would not be appropriate to subtract the preflare line strengths because the preflare source region would no longer exist; it would have been incorporated into the flare. This latter situation may exist at least at the end of the 1980 April 8 flare. Then, the inferred O VII flare volume would correspond to an angular dimension of at least 32 arcseconds, or more than half the spectrometer field of view. Inferred volumes late in the other two flares are small enough that the preflare background emission could have been undisturbed. The important point is that all three flares had a very small volume near the beginning of O VII emission, small enough that the assumption of an undisturbed preflare emission would appear to be a good one. Such a background should be subtracted from the total emission early in the flare. Doing this yields peak densities of the order of 10^{12} cm^{-3} , chromospheric densities, for all three events. This lends support to the model discussed above, in which the hot thermal plasma originates in the chromosphere and evaporates up into coronal loops to form a large, low-density source.

An argument which supports the interpretation of the results in terms of chromospheric evaporation is that in all three flares, sufficient energy is deposited at the loop footpoints by energetic electrons for explosive evaporation to occur. According to Fisher, Canfield, and McClymont

(1985), who have studied the balance between flare heating by a nonthermal population of electrons and radiative cooling of the plasma in the upper chromosphere, an energy flux greater than a certain threshold F_{crit} may cause the pressure in this plasma to increase, thereby causing an expansion of the plasma, and causing its temperature to rise to coronal values. Fisher, Canfield, and McClymont found that the threshold for the energy flux corresponding to a beam of electrons with cutoff energy at 20 keV is approximately $F_{crit} = 10^{10} \text{ erg cm}^{-2} \text{ s}^{-1}$. In Figures 11a, 11b and 11c, P_{elect} , the rate at which electrons deposit their energy into the loop footpoints, is plotted together with the associated volume as a function of time for the three events. P_{elect} was obtained from the power-law spectral analysis of the hard X rays, assuming thick target bremsstrahlung emission. In order to compare F_{crit} with P_{elect} , we estimated an upper limit to the required energy deposition rate by multiplying F_{crit} by the maximum value of the area associated with the microwave source, which is clearly an upper limit to the loop footpoint area. We found that P_{elect} exceeded even this upper limit to the threshold for all three flares. The horizontal line across each graph of Figure 11 indicates the value for which P_{elect} is large enough to satisfy the first of the two criteria for explosive evaporation to take place. This happens early in the impulsive part of each flare.

If, in addition to attaining the threshold, the heating takes place on a time scale shorter than the hydrodynamic expansion time scale of the plasma, the overpressure will be large enough for "explosive" evaporation to take place. This process is characterized by a significant change of the volume in a period less than one second. In order to determine if the rise of the heating rate is rapid enough that explosive evaporation is to be expected in a flare, Fisher (1987) compares this rise time of nonthermal electron heating to a time scale which depends on the initial thickness of the evaporating plasma and on the heating rate per particle. Fisher finds that in typical flares, the heating must occur on a time scale less than 0.7 s, for energy flux densities between 10^{10} and $5 \times 10^{11} \text{ erg cm}^{-2} \text{ s}^{-1}$. Figure 11 also shows that the e-folding time for P_{elect} to reach the threshold value F_{crit} is greater than 10 s in each flare. This rise time in the heating rate may explain why the evaporation is not explosive, and why the O VII source volume expands over a period of minutes. In their calculations, Fisher,

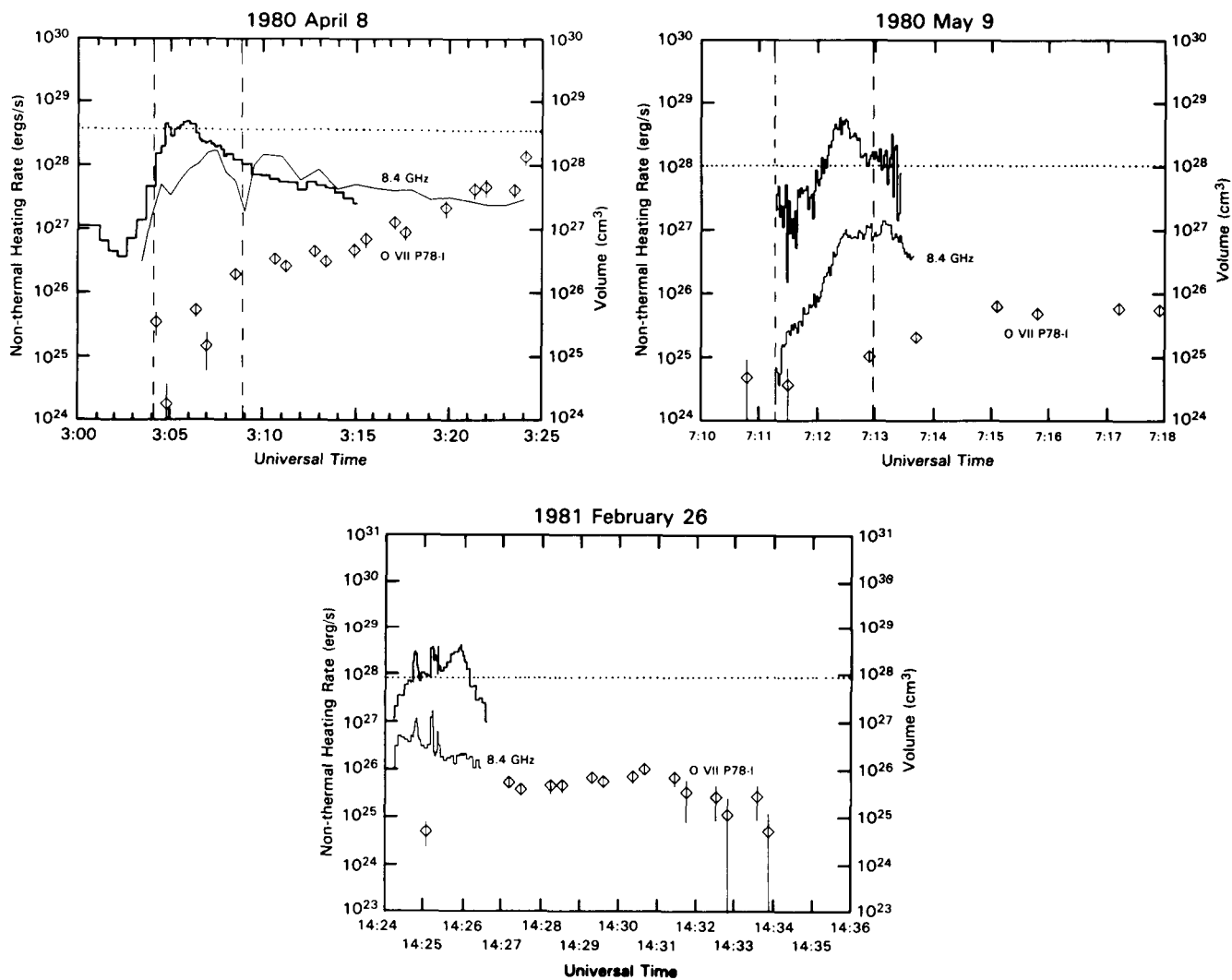


Figure 11. Energy flux into the loop footpoints, derived from the spectral analysis of the hard X rays under the assumption that the hard X-ray emission arose from a non-thermal population of electrons incident on a thick target. The energy flux is represented by the bold line curve in each of the figures. For comparison, the microwave source volume is also plotted in each figure. The volumes inferred from microwaves and hard X rays (thin line), and from the O VII line emission (diamonds) are also plotted functions of time for comparison. The horizontal line across the top of each graph represents an upper limit to the threshold energy flux necessary for the onset of explosive chromospheric evaporation. Top panel: Results for the 1980 April 8 flare. The vertical dashed lines indicate the time interval during which blue-shifts were measured in Ca XIX lines by Antonucci, Gabriel, and Dennis (1984). Middle panel: Results for the 1980 May 9 flare. The vertical dashed lines indicate the time interval during which blue-shifts were measured in Ca XIX and Fe XXV lines by Antonucci et al. (1982). Bottom panel: Results for the 1980 February 26 flare.

Canfield, and McClymont assume that the material in the chromosphere is heated by a beam of energetic electrons. A comparison of these observations with predictions of a model where the chromosphere is heated by a quasithermal population of electrons is beyond the scope of this study. Such a comparison bears looking into during future studies, given the success of a quasithermal model in describing other aspects of flare dynamics.

In comparing the volumes derived from the O VII spectra with those inferred from the hard X-ray/microwave analysis, we find that the O VII volumes during the impulsive phase of the flare are lower by several orders of magnitude. We have interpreted this difference to a localization of the O VII source at the flare footpoints, and associated it with the start of chromospheric evaporation.

We found that for all three flares, the O VII volume increases during the impulsive phase when we expect chromospheric evaporation to be taking place. However, it reaches a plateau that is still generally lower than the hard X-ray/microwave volume by a factor of about ten. At least part of this difference may be attributed to our use of A_{eff} as the estimator of the hard X-ray/microwave volume, rather than considering a more realistic loop geometry. One possible explanation of the remaining difference has already been suggested: that the O VII emission arose from a different loop than the hard X-ray/microwave source. This model is not very satisfactory, as it requires on the one hand that the chromosphere be heated as a result of an energy release that has taken place higher in the corona in the same magnetic flux tube; yet requires the heated material to enter a different flux tube in order to explain the volume difference.

An alternate possibility is that the loop is vertically stratified. According to this idea, strong heating would drive the formation region of the O VII lines downward into regions of higher density so that the 2.5×10^6 K plasma becomes an extension of the transition zone. During the evaporation phase, the rising material entering the loop would continue to be heated from above, eventually becoming too hot to emit O VII lines. The volume of the 2.5×10^6 K region would increase until it filled about ten percent of the loop height. During the gradual phase, the 2.5×10^6 K layer would be maintained by conduction from the hotter material higher in the loop. The idea of an extended transition zone is supported by loop

model calculations such as those of Nagai (1980). A difficulty with this explanation, however, is that it requires most of the 2.5×10^6 K plasma to be concentrated in a thin layer at the flare footpoints during the gradual phase of the flare; a situation that is not generally observed.

The volume difference also may be discussed in terms of a filling factor. Here, it is postulated that the loop system is comprised of distinct, separate parts which can be at different temperatures. The system might, for example, consist of a bundle of narrow strands (the spaghetti model) or a series of coaxial sheaths or shells (the shell model). In either case, the hard X-ray/microwave results represent the volume of space inside the surface in which the microwave optical depth is unity. In the shell model, the O VII emission would be confined to a sheath (Bruner *et al.*, 1983), the volume of which was about 10 % of the total. In the spaghetti model, O VII would fill a subset of the strands whose combined volume is likewise 10 % of the total. In either case, the different temperature regions are thermally isolated from each other by the magnetic field. The magnetic field will also supply a component of pressure so that the differing temperature regions need not be in hydrostatic equilibrium with one another.

During each flare studied here, blue-shifts were observed by other authors in emission lines of ions corresponding to higher temperatures than O VII. For the 1981 February 26 flare, Feldman (private communication) reports velocities of 320 km s^{-1} in Ca XIX lines, measured as early as 14:24:40 UT with the SOLFLEX spectrometer on board *P78-1*. In their study of the flares of 1980 April 8 and 1980 May 9, Antonucci *et al.* (1982) and Antonucci, Gabriel, and Dennis (1984) report observations of high blue-shifts in Ca XIX and Fe XXV emission lines. They interpret these in terms of Doppler shifts due to chromospheric evaporation. In the case of the April 8 flare, the velocities inferred from shifts in Ca XIX lines are between 100 km s^{-1} and 300 km s^{-1} . For the May 9 flare, the velocities inferred from the calcium and iron lines are approximately 285 km s^{-1} and 430 km s^{-1} , respectively. The time intervals during which these blue-shifts were observed are indicated in Figures 11a and 11b. The fact that these intervals correspond approximately to the times when the O VII source volume was in expansion suggests that these phenomena are manifestations of a common process. The uncertainties in the data do not allow us to make

a statement about the relative timing in the case of the 1980 May 9 and 1981 February 26 flares.

Within the limits of the spectral resolution of the oxygen data, it is possible to rule out any velocity greater than 250 km s^{-1} , which is about the ion sound speed of the $2 \times 10^6 \text{ K}$ plasma. No blue-shift was measurable in the O VII lines for any of the flares discussed here. This is not surprising because material at these temperatures is just beginning to accelerate and would not yet have reached high velocities.

5 SUMMARY

For each of the three flares, we have calculated the volume of the flaring region by two independent methods, one characterizing the very hot plasma that exhibits the impulsive behavior seen in microwaves and in hard X-ray radiation, and the other characterizing the 2×10^6 K plasma of the gradual phase. There are striking similarities in the time evolution of the derived volumes for the three flares, and in the relationships between the two temperature regimes, which evolve in quite different ways. We summarize our results in the following points:

1. The volume of the impulsive microwave source follows the same evolution in each flare. The volume rises rapidly, roughly in proportion to the microwave flux, and reaches maximum at about the time of peak microwave flux. We have interpreted this rise in terms of a mechanism, such as a conduction front propagating along the confining magnetic loop, that produces an increase in the volume of energetic electrons corresponding to an increase in the impulsive emissions.
2. Results of our impulsive source volume calculations are essentially the same, whether it is assumed that the hard X rays are due to thermal bremsstrahlung emission or to thick target emission from a power-law population of electrons. Moreover, the results are in reasonable agreement with measurements of flare sizes obtained with HXIS and FCS.
3. Initially, the O VII source volume is smaller than the impulsive source volume by two to three orders of magnitude. As the gradual phase evolves, the volume of the O VII source increases, approaching (but not reaching) that of the microwave source. We have argued that the O VII source is initially confined to the loop footpoints, and have attributed the subsequent increase to the chromospheric evaporation mechanism. This interpretation is supported by two additional pieces of observational evidence: a) the electron population inferred from the impulsive emissions could provide an energy flux large enough to cause chromospheric evaporation; and b) strong blue-shifts are visible in other hot X-ray emission lines such as Ca XIX and Fe XXV, during

approximately the same interval when the O VII source volume is seen to expand.

4. The O VII source volume remains below the peak value of the impulsive source volume throughout each of the flares, reaching values of the order of 10 to 50 %, depending on the geometry assumed for the microwave source. We have discussed this difference in terms of filling factors in a loop system geometry consisting either of multiple strands (the spaghetti model) or of nested shells.
5. The areas of the soft X-ray sources in the $3-10 \times 10^6$ K temperature range could be derived from observations with the *SMM* FCS for the 8 April flare. They were found to be comparable to the area of the microwave source, and showed a trend of increasing area with decreasing temperature.

REFERENCES

- Antonucci E., Gabriel A. H., Acton L. W., Culhane J. L., Doyle J. G., Leibacher J. W., Machado M. E., Orwig L. E., Rapley C. G., 1982, Solar Phys., **78**, 107.
- Antonucci E., Gabriel A. H., Dennis B. R., 1984, Ap. J., **287**, 917.
- Batchelor D. A., 1984, "Energetic Electrons in Impulsive Solar Flares" Ph.D. Dissertation, University of North Carolina, Chapel Hill, NASA Technical Memorandum 86102.
- Batchelor D. A., Cranell C. J., Wiehl H. J., Magun A., 1985, Ap. J., **295**, 258.
- Brown J. C., 1971 Solar Phys. **18**, 489.
- Brueckner G., 1976, Phil. Trans. R. Soc. London A, **281**, 443.
- Bruner, M. E., Brown W. A., Acton L. W., Strong K. T., 1983, Bull. Am Astr. Soc., **18**, 708.
- Cranell C. J., Frost K. J., Matzler C., Ohki K., Saba J. L. 1978, Ap. J., **223**, 620.
- Colgate, S., 1978, Ap. J., **221**, 1068.
- Dennis B. R., 1982, "HXRBS Spectral Analysis", unpublished technical report.
- Doschek G. A., Feldman U., Landecker P. B., McKenzie D. L., 1981, Ap. J., **249**, 372.
- Dulk G., Marsh K. A., 1982, Ap. J., **259**, 350.
- Feldmann U., Doschek G. A., Kreplin R. W., Mariska J. T., 1980, Ap. J., **241**, 1175.
- Fisher G. H., 1987, Ap. J. **317**, 502.
- Fisher G. H., Canfield R. C., McClymont A. M., 1985, Ap. J., **289**, 425.
- Gary D. E., 1985, Ap. J., **297**, 799.
- Hoyng P., Brown J. C., van Beek H. F., 1976, Solar Phys., **48**, 197.

- Keenan F. P., Tayal S. S., Kingston A. E., 1984, Solar Phys., 92, 75.
- Lin R. P., Hudson H. S., 1976, Solar Phys., 50, 153.
- Machado M. E., 1983, Solar Phys., 89, 133.
- Machado M. E. , Somov B. V., Rovira M. G., De Jager C., 1983, Solar Phys., 85, 157.
- Mätzler Ch., 1978 , Astron. Astrophys., 70, 181.
- Magee N. H. , Jr., Mann J. B., Merts A. L., Robb W. D., 1977, Los Alamos report LA-6691-MS.
- Orwig L. E., Frost K. J., Dennis B. R., 1981 Ap. J. (Letters), 244, L163.
- Pradhan A. K. , 1982, Ap. J., 263, 477.
- Schoechlin W., Magun A., 1979, Solar Phys., 64, 349.
- Starr R., Heindl W. A., Crannell C. J., Thomas R. J., Batchelor D. A., Magun A., 1987, "Energetics and Dynamics of Simple Impulsive Solar Flares." Submitted to The Astrophysical Journal for publication.
- TFR Group, Doyle J. G., Schwob J. L., 1982, J. Phys. B., 15, 813.
- Van Hoven, G., 1981, "Solar Flare Magnetohydrodynamics", ed. E. R. Priest, Gordon and Breach, New York, Chapter 4.
- Wu S. T., de Jager C., Dennis B. R., Hudson H. S., Simnett G. M., Strong K. T., Bentley R. D., Bornmann P. L., Bruner M. E., Cargill P. J., Crannell C. J., Doyle J. G., Hyder C. L., Kopp R. A., Lemen J. R., Martin S. F., Pallavicini R., Peres G., Serio S., Sylwester J., and Veck N. J., "Energetic Phenomena on the Sun" 1986, ed. B. E. Woodgate and Kundu M. R., NASA CP 2439, Chapter 5.
- Zarro D. M., Strong K. T., Canfield R. C., Metcalf T., Saba J. L., 1987, Adv. Space Res., in press.



Report Documentation Page

1. Report No. NASA TM-87815		2. Government Accession No.		3. Recipient's Catalog No.	
4. Title and Subtitle Dynamic Evolution of the Source Volumes of Gradual and Impulsive Solar Flare Emissions				5. Report Date December 1987	
				6. Performing Organization Code 682	
7. Author(s) M. E. Bruner, C. J. Crannell, F. Goetz, A. Magun, and D. L. McKenzie				8. Performing Organization Report No. 88B0077	
				10. Work Unit No.	
9. Performing Organization Name and Address Goddard Space Flight Center Greenbelt, Maryland 20771				11. Contract or Grant No.	
				13. Type of Report and Period Covered Technical Memorandum	
12. Sponsoring Agency Name and Address National Aeronautics and Space Administration Washington, D.C. 20546-0001				14. Sponsoring Agency Code	
15. Supplementary Notes M. E. Bruner is affiliated with Lockheed Palo Alto Research Laboratory, Palo Alto, California; A. Magun is affiliated with the Institute for Applied Physics, University of Bern, Bern, Switzerland; D. L. McKenzie is affiliated with the Space Sciences Laboratory, The Aerospace Corporation, Los Angeles, California; and C. J. Crannell and F. Goetz are affiliated with NASA/Goddard Space Fl. Center.					
16. Abstract This study compares flare source volumes inferred from impulsive hard X rays and microwaves with those derived from density sensitive soft X-ray line ratios in the O VII spectrum. The data for this study were obtained with the SMM Hard X-Ray Burst Spectrometer, Earth-based radio observatories, and the SOLEX-B spectrometer on the P78-1 satellite. Data were available for the flares of 1980 April 8, 1980 May 9, and 1981 February 26. The hard X-ray/microwave source volume is determined under the assumption that the same electron temperature or power law index characterizes both the source of hard X rays and the source of microwaves. The O VII line ratios yield the density and volume of the 2×10^6 K plasma. For all three flares, the O VII source volume is found to be smallest at the beginning of the flare, near the time when the impulsive hard X-ray/microwave volume reaches its first maximum. At this time, the O VII volume is three to four orders of magnitude smaller than that inferred from the hard X-ray/microwave analysis. Subsequently, the O VII source volume increases by one or two orders of magnitude, then remains almost constant until the end of the flare when it apparently increases again. The results are discussed in terms of the chromospheric evaporation process.					
17. Key Words (Suggested by Author(s)) Sun: Flares Sun: Microwaves Sun: X Rays Sun: Chromospheric Evaporation			18. Distribution Statement Unclassified - Unlimited Subject Category 92		
19. Security Classif. (of this report) Unclassified		20. Security Classif. (of this page) Unclassified		21. No. of pages 42	22. Price A03